Understanding teleconnections with the Indo-Pacific region during the northern winter

Franco Molteni, Tim Stockdale and Frederic Vitart

ECMWF, Reading, U.K.

1 Introduction

For many years, scientists working on dynamical seasonal predictions have looked at the El Nino - Southern Oscillation (ENSO) phenomenon as the predominant source of predictability, as clearly shown in the review papers collected by Anderson et al. (1998) to showcase the achievements of the Tropical Ocean - Global Atmosphere (TOGA) programme. The importance of ENSO and the associated teleconnections originating from the central and eastern tropical Pacific is, of course, well recognized today as it was 15 years ago. However, the scientific community has realized that skilful seasonal predictions for most extratropical regions, as well as parts of the tropics, cannot be achieved unless the variability originated from other ocean basins is properly understood and modelled.

The tropical West Pacific and Indian Oceans are closely connected to the 'classical' El Nino domain, and links between the variability occurring in different parts of the full Indo-Pacific region have been investigated by many authors. The importance of Indian Ocean variability as a source of planetary-scale teleconnections was highlighted in the late 1990's and early 2000's by the identification of the Indian Ocean Dipole (Saji et al. 1999; Webster et al. 1999) and by the numerical simulation of a link between trends in Indian Ocean sea-surface temperature (SST) and interdecadal variability of the North Atlantic Oscillation (NAO) (e.g. Hurrell at al 2004; Hoerling et al. 2004). ENSO teleconnections are also affected by co-occurring anomalies in the tropical Indian Ocean: in a study performed with two different atmospheric general circulation models (AGCMs) forced by prescribed SST, Annamalai et al (2007) claimed that the effect of Indian Ocean SST during El Nino episodes was partially compensating the signal originated from the central and eastern Pacific, leading to a reduced amplitude of the atmospheric response in the North Pacific / North American region.

Results on Indian-West Pacific teleconnections obtained with AGCM simulations have been questioned by a number of authors. Wang et al. (2005) showed that air-sea interactions in the Eastern Indian and West Pacific region during the boreal summer were incorrectly simulated by AGCMs, and that seasonal predictions of the Asian monsoon require the use of coupled GCMs for a proper simulation of the links between

SST and rainfall anomalies. The realism of the AGCM response to Indian Ocean warming was questioned by Copsey et al. (2006), while Kucharski et al. (2006) argued that SST anomalies in the equatorial and sub-tropical West Pacific are also connected with wintertime NAO variability on the decadal scale.

In recent years, the interest in connections between the Indo-Pacific and North Atlantic region has been shifted from the decadal to the intra-seasonal time scale, with a focus on the impact of the diabatic heating anomalies associated with the Madden-Julian Oscillation (MJO). Cassou (2008) investigated the impact of MJO variability on the frequency of North Atlantic flow regimes in the observational record, and the associated teleconnection were reproduced in the studies by Lin et al. (2009) and Vitart and Molteni (2010).

What about the seasonal-mean scale, and the impact on seasonal predictability? One might argue that a seasonal average tends to wipe out the signal associated with MJO variability (which has the largest signal in the 40-to-60 day range), while the effects of interdecadal changes explain a small fraction of variance. However, provided a significant anomaly in diabatic heating persisted throughout a season, there are no reasons why the dynamic processes which originate the extratropical response to Indian and West Pacific anomalies on either shorter or longer time scales should not manifest themselves on the seasonal scale.

The goal of this paper is to investigate the teleconnection patterns originated from the Indian-West Pacific region during the boreal winter in both the observational record and in the set of seasonal ensemble simulations performed to calibrate the latest ECMWF seasonal forecast system (System 4; see Molteni et al. 2011). Specifically, we argue that the comparison between observed and model data provides a clearer understanding of whether extratropical anomalies are linked to rainfall, rather than SST, variability. Why this should be the case will be discussed in the next section, which will also describe the statistical methodology, available datasets and model configuration. In Section 3, we present the results of our comparison between observed and modelled teleconnections. In section 4, implications for seasonal predictions and the consistency of signals across different time scales are discussed, and a summary of our findings is given in section 5.

2 Motivation and methodology

2.1 Open issues on Indo-Pacific teleconnections

The main assumption behind seasonal prediction is that the 'signal' to be predicted is primarily originated by variations in the 'slow' component of the climate system, such as the ocean, land-surface and sea ice, while the internal variability of atmosphere is responsible for most of the 'noise' which has little or no predictability on seasonal scales. Among these slow components, it is also accepted that the tropical oceans play the most important role as sources of seasonal predictability. As a result, teleconnection studies aimed at understanding seasonal variability and predictability have often been based on correlations between SST anomalies in specific tropical regions and variations in atmospheric circulation patterns.

In the Indo-Pacific region, the relationship between SST in the Indian and Pacific basins show a clear seasonal dependency. This is summarized in Figure 1, taken from the review by Schott et al. (2009), which illustrates the relationship between SST anomalies associated with ENSO and SST variability in the western and eastern Indian ocean. It highlights the fact that, when looking at SST, the so-called Indian Ocean Dipole is mainly a boreal autumn phenomenon: only in this season a clear anti-correlation is present between the western and eastern side of the Indian Ocean, with the two regions having opposite relationship with the central Pacific. Conversely, during the boreal winter, SST across the whole tropical Indian Ocean tends to be the same sign, and be positively correlated with El Nino anomalies. As a consequence, while studies on the teleconnections of the Indian Ocean Dipole (mainly during late summer and autumn) have made a clear distinction between signal coming from the western and eastern side of the tropical Indian Ocean, such a distinction is usually neglected when wintertime Indo-Pacific teleconnections are investigated. For example, in the AGCM experiments by Annamalai et al. (2007), the Indo-Pacific region is separated in two domains with a boundary at 120E, so that their Indian Ocean domain ranges from the eastern Africa coast to the longitude of Borneo. However, at the beginning of their paper, the authors point out (see their Figure 2) that even during the boreal winter season the western and eastern part of the Indian Ocean behave differently in terms of correlation of SST with either rainfall or thermocline depth. Notably, correlation between SST and rainfall is weak or negative in the eastern Indian Ocean, especially in the region west of Sumatra.

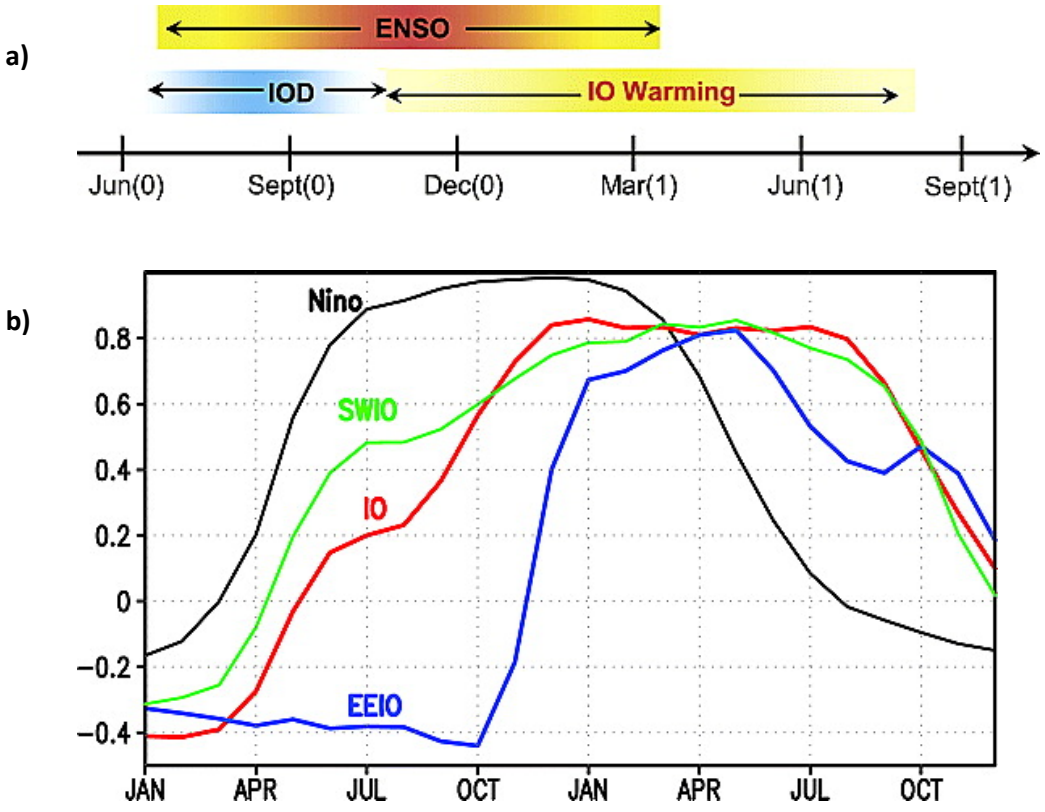

Figure 1a) Connections between SST variability in the Indian Ocean associated with warm ENSO events (El Nino). IOD refers to the Indian Ocean Dipole. b) Lag correlation between SST in the Nino3.4 region in November and SST in the whole tropical Indian Ocean (IO), south-western Indian Ocean (SWIO) and eastern equatorial Indian Ocean (EEIO). Reproduced from Schott et al. (2009).

Discussing the seasonal predictability of the Asian monsoon, Wang et al. (2005) pointed out that ACMs are unable to reproduce correctly the rainfall variability in regions where the correlation between rainfall and SST is negative, ie where SST variability is mainly the result of radiative and evaporation feedbacks associated with tropical convection. The same argument should be applied to study of wintertime teleconnection: for example, prescribing a near-uniform SST warming across the whole tropical Indian Ocean tends to produce a zonally coherent precipitation response in AGCM experiments (see Sect. 4.3), which is not consistent with negative SST-rainfall correlation in the eastern part of the ocean. Therefore, a modelling assessment of Indo-Pacific teleconnections should rather be carried out using coupled models, and a distinction between western and eastern Indian Ocean should also be made during the winter season.

2.2 Observational datasets and model simulations

To investigate the issues discussed above, in the next section we compare teleconnection patterns computed from observed data (or re-analyses) and from ensemble re-forecast experiments. Observational datasets come from two sources. For upper-air atmospheric fields and SST, we use the monthly-mean products from the ECMWF ERA-Interim re-analysis (Dee et al. 2011), which has recently been extended from January 1979 to near-real time. For precipitation, we use the GPCPv2.2 monthly means, available from January 1979 to December 2010.

Model data are taken (again as monthly means) from the re-forecast archive generated for the calibration of the latest ECMWF seasonal forecast system, referred to as System 4. A detailed description of the system, the coupled-model biases and the (estimated) predictive skill is given in Molteni et al. (2011). Here, we summarize a few essential characteristics of the coupled model and the re-forecast set.

- The coupled model is composed of a recent version of the ECMWF atmospheric model (IFS cycle 36r4) and the NEMO ocean model (Madec 2008), coupled via the OASIS3 coupler developed by CERFACS (Valcke 2013).
- The atmosphere model has a spectral truncation at T255 (equivalent to approx. 80km resolution in the horizontal) and 91 vertical levels; the NEMO model is used in its ORCA-1 configuration, with resolution of about 1 degree in the extratropics and an equatorial refinement to 1/3-degree latitude, and 42 vertical levels.
- The re-forecast experiments consist in 15-member ensembles started on the 1st of each month from January 1981 to December 2010, with a duration of 7 months (extended to 13 months every quarter-year). Initial data come from ERA-Interim for the atmospheric part and from the ORA-S4 ocean re-analysis performed with the NEMOVAR 3D-var system (Balmaseda et al. 2013).

Since in this study we focus on the boreal winter period, 3-month means for the December-January-February (DJF) period will be computed. For the re-forecast experiments, these data will be taken from the experiments started on 1 November 1981 to 2010, and correspond to the month 2-to-4 forecast range. Verification fields are available for the whole 30-year period, with the exception to GPCP data for January

and February 2011 (corresponding to forecast months 3 and 4 for the start date of Nov. 2010). In order to make use the full 30-year record, rainfall anomalies for these 2 months are estimated from a regression of the 2.5-degree GPCP data against the ERA-interim monthly rainfall, aggregated onto the GPCP grid and based on the 1979 to 2010 record.

2.3 Statistical analysis

Since we argued that it is important to look separately at regions with different local correlation between SST and rainfall, the first task is to verify that such regions can be identified in a consistent way in both our observational and model datasets. Fig. 2a shows the local (ie grid-point) correlation between ERA-Interim SST and GPCP rainfall anomalies for DJF in the Indo-Pacific domain; fig. 2b shows the corresponding map derived from the System-4 re-forecasts, where correlations are computed treating each ensemble member as a separate realization.

Looking at the near-equatorial belt, regions of large positive correlation can be found in the western-to-central Indian Ocean and the central-to-eastern Pacific in both observed and model data. For these regions, it is fair to assume that SST variability 'forces' rainfall (and hence diabatic heating) anomalies of the same sign. Instead, in the eastern Indian Ocean and the seas surrounding the Maritime Continents, especially south of the Equator, SST-rainfall correlation is either weakly positive or negative. Again, the model simulations show a good consistency with observations.

For simplicity, we prefer to use areas of equal size, located in the same latitudinal band (10N-10S) to quantify the sources of teleconnections. These areas are highlighted by coloured boxes in Fig. 2. One area (from 40E to 90E) covers the western and central Indian Ocean (WCIO), where SST-rainfall correlation is moderately large and positive. The second area includes goes from the eastern Indian Ocean to the western edge of the Pacific (EIWP: 90E-140E) and includes regions where SST-rainfall correlation is weak and/or negative. The third area corresponds to the NINO4 longitudinal domain (160E-150W); because of the wider latitudinal extent (20 degrees instead of 10), we refer to this area as NINO4W. This latter area is characterized by a strong positive correlation between SST and rainfall, and is arguably the stronger source of atmospheric teleconnection on the seasonal time scale.

In the following sections, we quantify teleconnections by showing regression maps of rainfall anomalies on a global domain and 500-hPa geopotential height anomalies over the northern hemisphere against time series of SST and rainfall averaged over the three areas selected above. The regression maps are scaled in such a way to represent the anomaly associated with a +1 standard deviation in the 'predictor' time series: this is equivalent to computing the covariance of the 'predictand' with the standardized time series of SST or rainfall averaged over the WCIO, EIWP and NINO4W regions. Again, individual ensemble members are treated as separate realizations of our 30-year sample; the amplitude of the regression map is therefore comparable between observation and model data. When re-forecast time series are compared against observations, both single-member and ensemble-mean data will be shown; predictive skill will be quantified by the anomaly correlation between the ensemble-mean time series and the ERA or GPCP data.

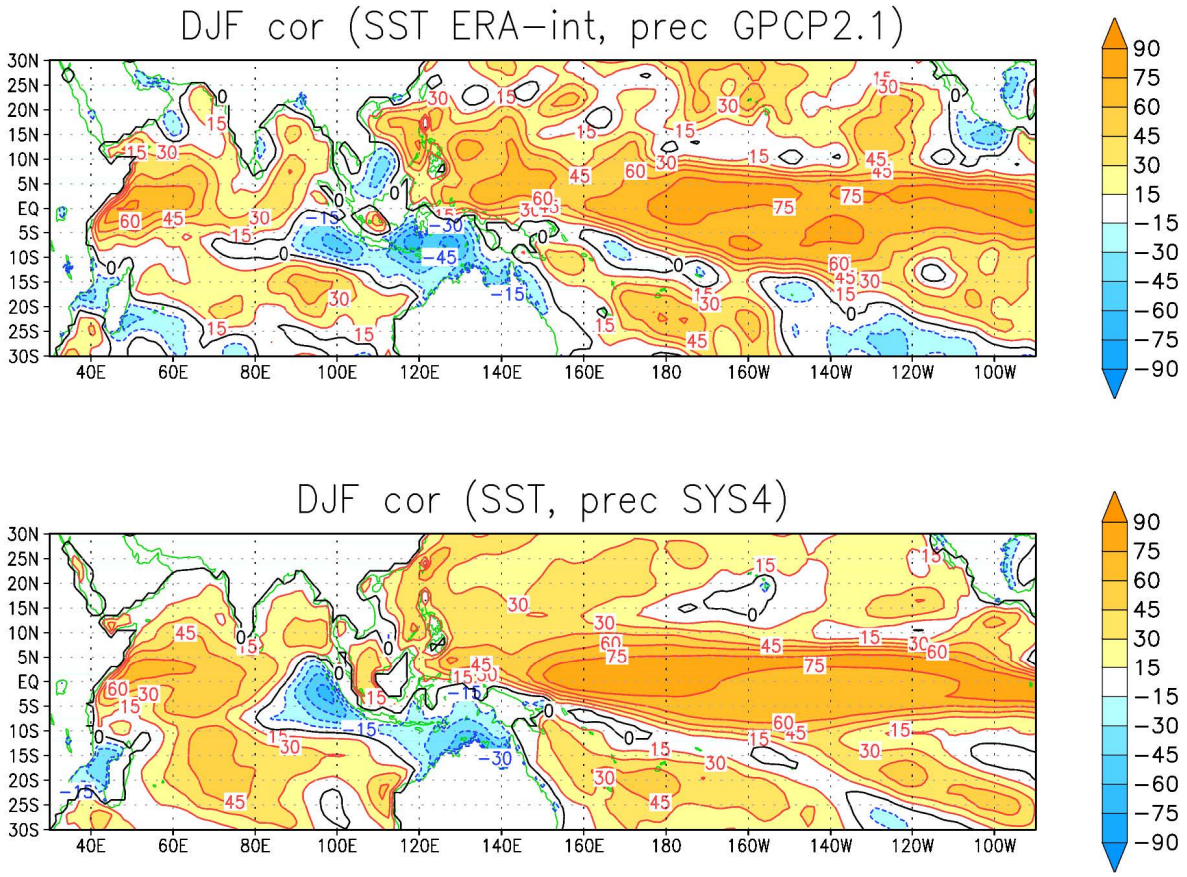

Figure 2 Local correlation between DJF rainfall and SST from ERA-Interim and GPCP data (top), and System-4 re-forecasts (bottom). The areas used to compute SST and rainfall anomalies in this paper are highlighted: Western-to-Central Indian Ocean (WCIO), Eastern Indian-Western Pacific (EIWP), "wide" Nino-4 region (NINO4W). Note that local SST-rainfall correlation is weak or negative in EIWP.

3 Teleconnections diagnosed from observed and model data

The first aspect to be investigated is how SST and rainfall anomalies in the WCIO, EIWP and NINO4W area co-vary with the same variable on a global domain.

3.1 Covariances with tropical SST and rainfall

Fig. 3 shows the covariance maps for SST for the three regions above computed from ERA-interim data, while fig. 4 shows the corresponding maps for System-4. The maps from ERA data confirm well-known relationships between Indian and pacific SST, with a clear positive correlation between SST in WCIO and in the central and eastern tropical Pacific. As noted above, in terms of SST anomalies the EIWP area is weakly but positively correlated with the rest of the tropical Indian Ocean, and with the eastern tropical Pacific. However, the covariance of north Pacific SST with the EIWP and NINO4W areas show nearly opposite patterns. The SST covariances from System-4 (fig. 4) reproduce most of the observed features in the tropical Indo-Pacific, albeit with a slightly stronger correlation between WCIO and the central Pacific. In the North Pacific, the connections with the El Nino signal is well reproduced, while the connection with EIWP SST is much weaker than observed.

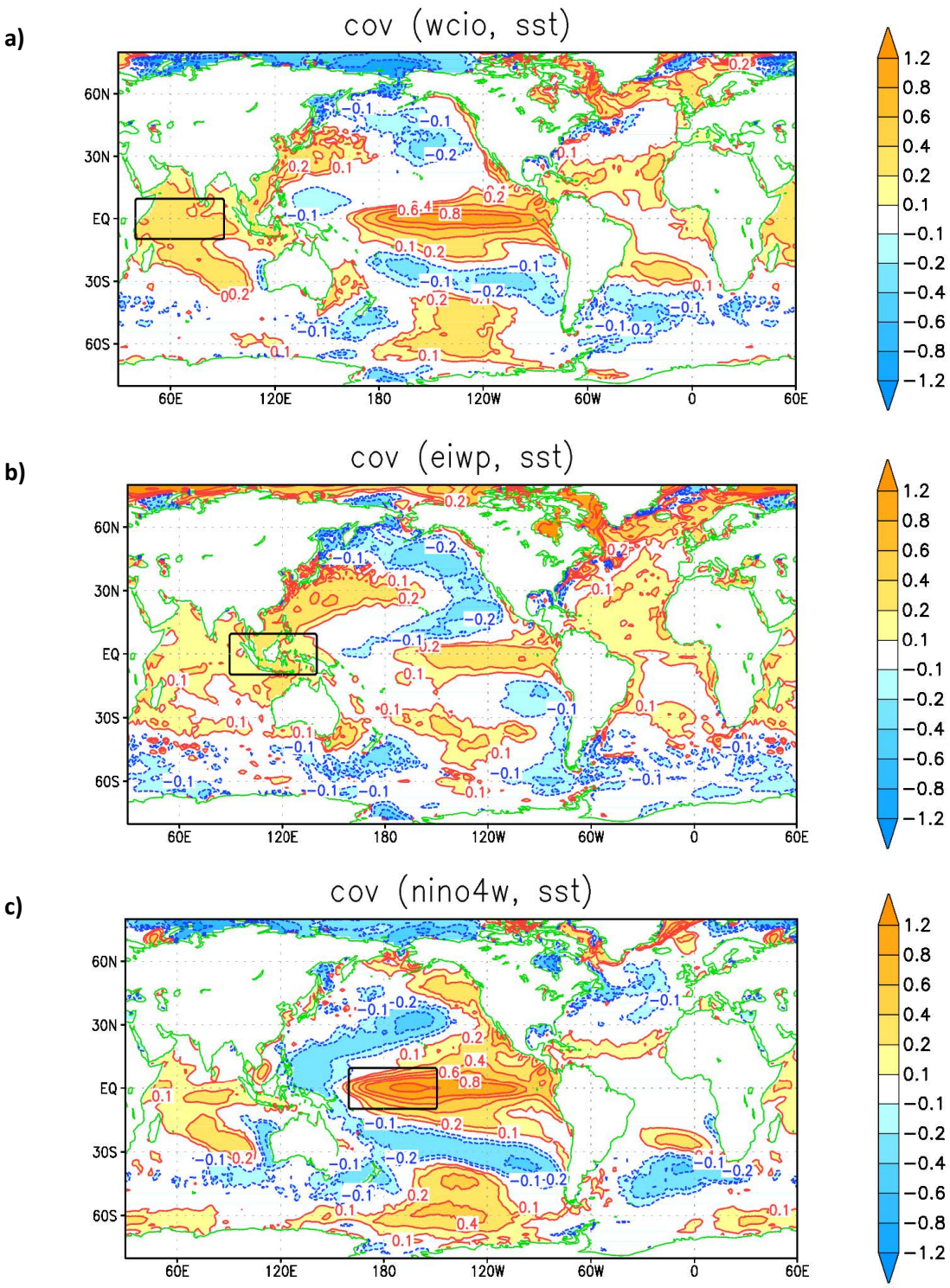

Figure 3 Covariance of DJF SST with the standardized SST anomaly in the WCIO (a), EIWP (b) and NINO4W (c) regions, shown by black boxes. Data from ERA-Interim.

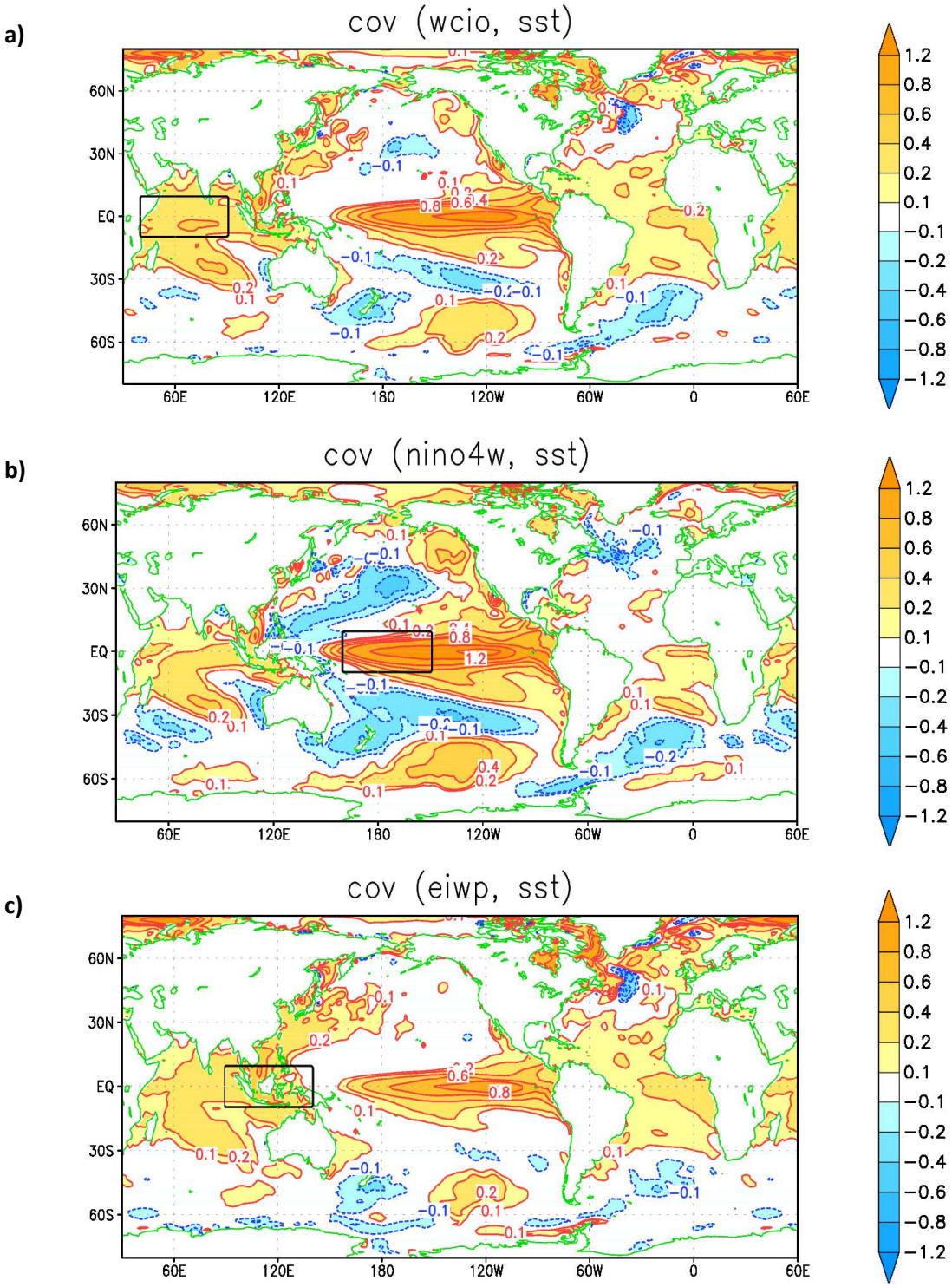

Figure 4 As in Fig. 3, but computed from System-4 re-forecasts started on 1 Nov. 1981-2010.

The equivalent covariance maps for rainfall are shown in Fig. 5 for GPCP and in Fig. 6 for System-4. Here, the anti-correlation between anomalies in EIWP and in the other two regions becomes evident, with a tri-polar anomaly pattern showing the same sign in WCIO and NINO4W. When looking at GPCP data, the WCIO covariance map shows comparable amplitude between the western Indian and central Pacific regions, while in System-4 the central Pacific covariance is larger than the signal over the WCIO area.

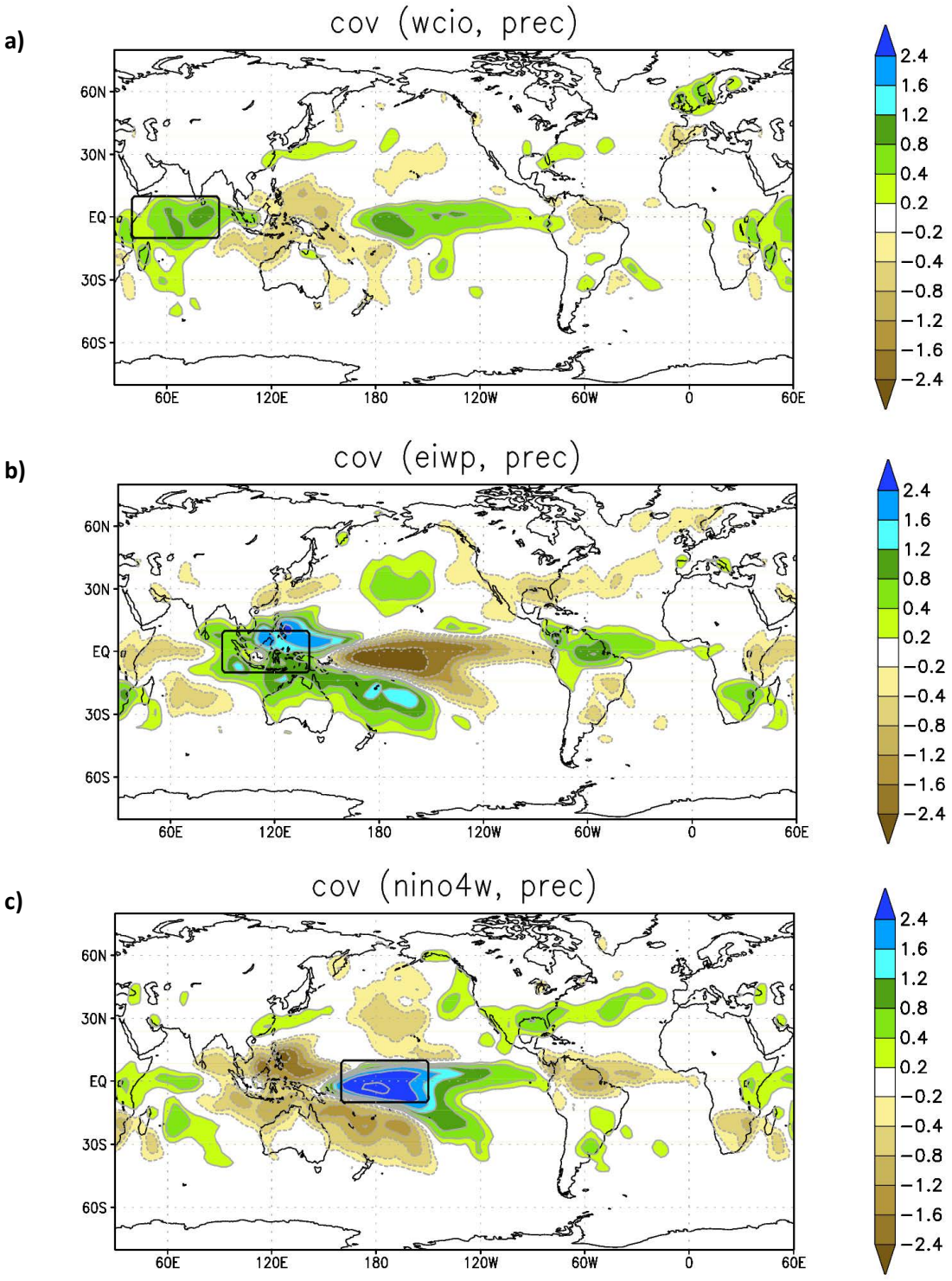

Figure 5 Covariance of DJF rainfall with the standardized rainfall anomaly in the WCIO (a), EIWP (b) and NINO4W (c) regions, shown by black boxes. Data from GPCP v2.2.

In other words, the rainfall covariance maps for WCIO and NINO4W tend to resemble each other more in System-4 than they do in GPCP data, again suggesting a stronger connection between Western Indian and central Pacific variability than the one implied by observed data. Apart from this, the simulation of rainfall covariances by System-4 looks very satisfactory when compared to GPCP results.

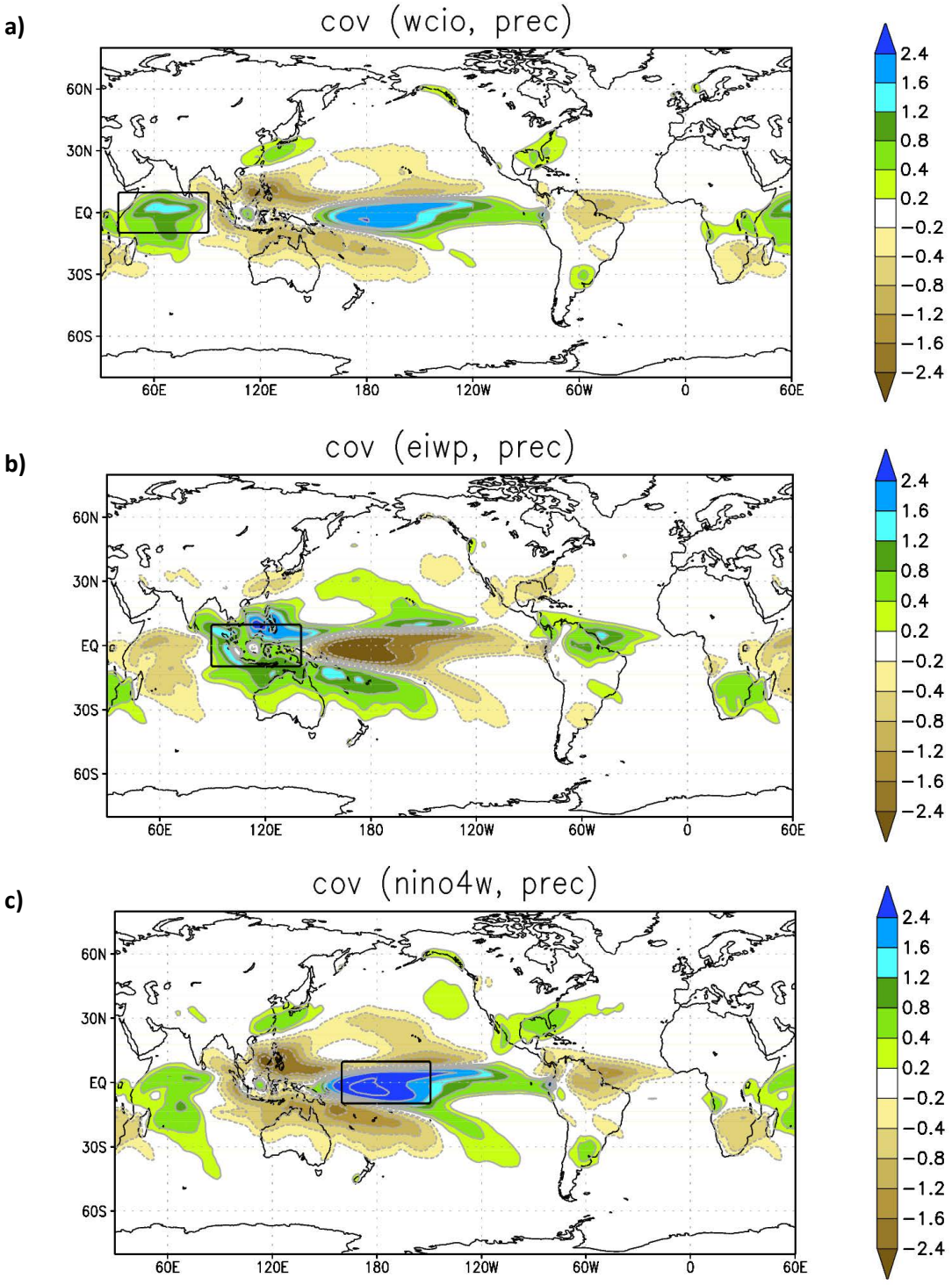

Figure 6 As in Fig. 5, but computed from System-4 re-forecasts started on 1 Nov. 1981-2010.

3.2 Connections between tropics and northern extratropics

We shall now explore the connection between the tropical Indo-Pacific regions and the northern extratropical circulation looking at covariances of the tropical signals with 500-hPa anomalies in DJF. In Fig. 7, the height field is regressed against the standardized SST anomalies in WCIO, EIWP and NINO4W, with the left column showing results from ERA-interim and the right column those from System-4.

Looking at the observed covariances in panels 7a-c, a strong similarity is evident between the patterns associated with positive SST anomalies in WCIO and NINO4W, although the former shows a stronger positive signal over the sub-tropical West Pacific. Over the North Pacific and North America, the classical features of the response to ENSO dominate the patterns, with negative anomalies in the region of the Aleutian low and south-eastern USA, and positive anomalies over Canada. Note that the extensions of the latter anomalies into the North Atlantic have a weak but negative projection onto the NAO. The covariance of 500-hPa height with the EIWP SST (panel 7b) shares some features with the covariance from the adjacent regions, but the anomaly in the Aleutian region is much weaker and confined to the northern latitudes.

The System-4 covariances in Fig. 7d-f give a contrasting message. Whereas the signal from the NINO4W region is realistically reproduced, the covariance from WCIO has about half the observed amplitude over the Pacific and is further reduced over North America, with almost no signal left over the North Atlantic. SST anomalies in EIWP do not appear to be associated with any significant signal in extra-tropical height, apart from a high-latitude wavenumber-2 pattern and a positive anomaly over Japan. At first glance, the discrepancies between the observed and modelled teleconnections from SST in WCIO and EIWP may suggest either a poor statistical significance of the observed signal, or a substantial model failure in simulating tropical-extratropical interactions originated from these regions.

Actually, although neither sampling errors nor model deficiencies can be neglected, a more fundamental reason for the discrepancies shown above is that the SST exert a much weaker “control” over the diabatic heating anomalies in WCIO and particularly in EIWP than they do over the core ENSO regions in central and eastern Pacific. This is confirmed by looking at covariances of extra-tropical 500-hPa with rainfall anomalies in the 3 tropical areas, shown in Fig. 8 using the same format of Fig. 7. If for the NINO4W region the observed and model covariances are again consistent and almost identical to those associated with SST anomalies, the similarity between observed and model results is much stronger for the signal originated from WCIO and EIWP rainfall, in both phase and amplitude. Specifically, a large positive response to above-average rainfall over EIWP is present over the North Pacific in both Fig. 8b and 8e. Also, the observed response to above-average rainfall over WCIO shows a clear positive NAO signal, which together with the related North Pacific anomalies resembles the Cold-Ocean-Warm-Land pattern described by Wallace et al. (1996). The positive NAO signal associated with WCIO rainfall is also simulated in the System-4 re-forecasts, although with a reduced amplitude.

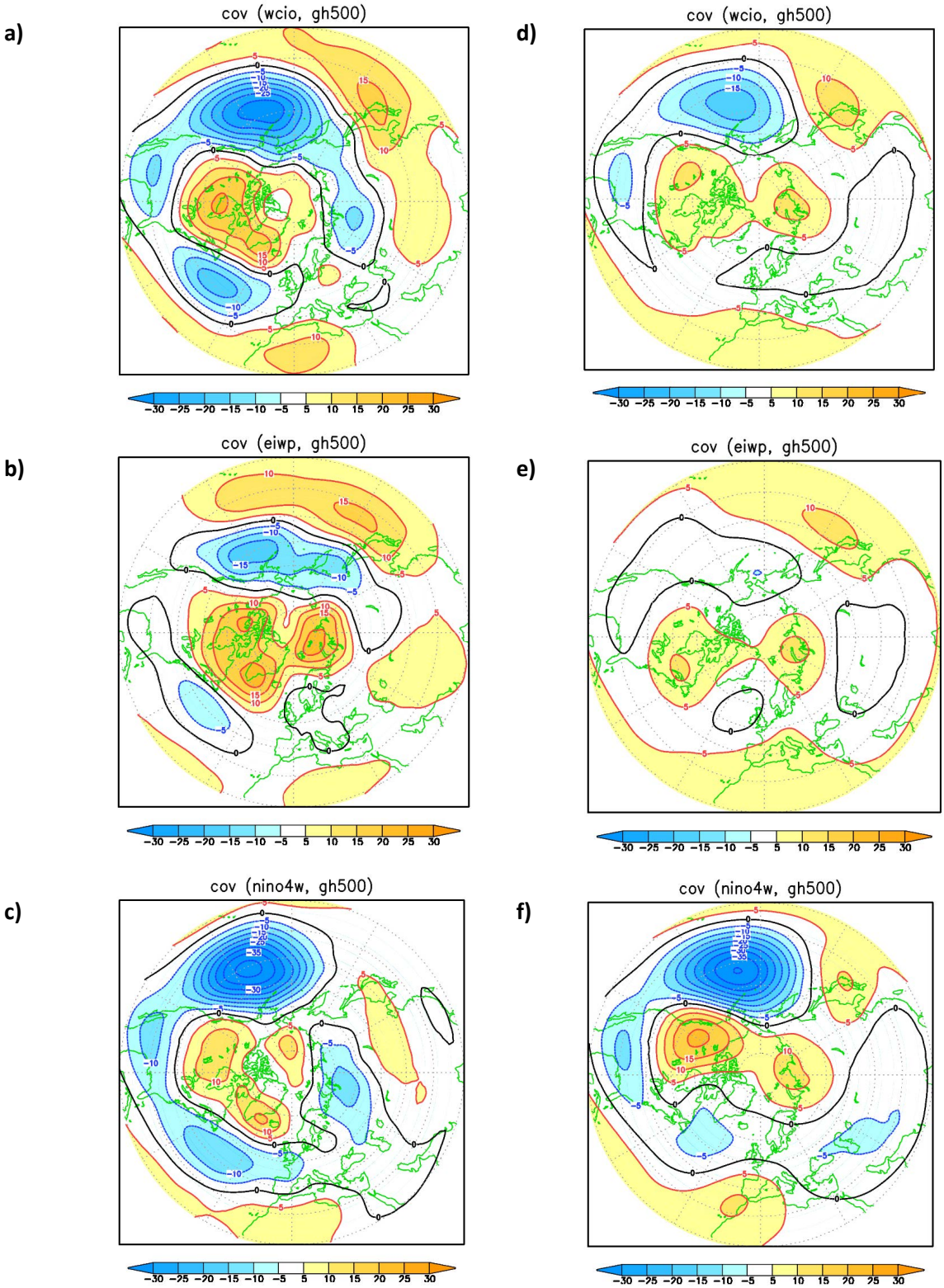

Figure 7 Covariance of DJF 500-hPa height with the stand. SST anomaly in the WCIO (a), EIWP (b) and NINO4W (c) regions. Data from ERA-Interim. (d) to (f): as in (a)-(c), but from System-4.

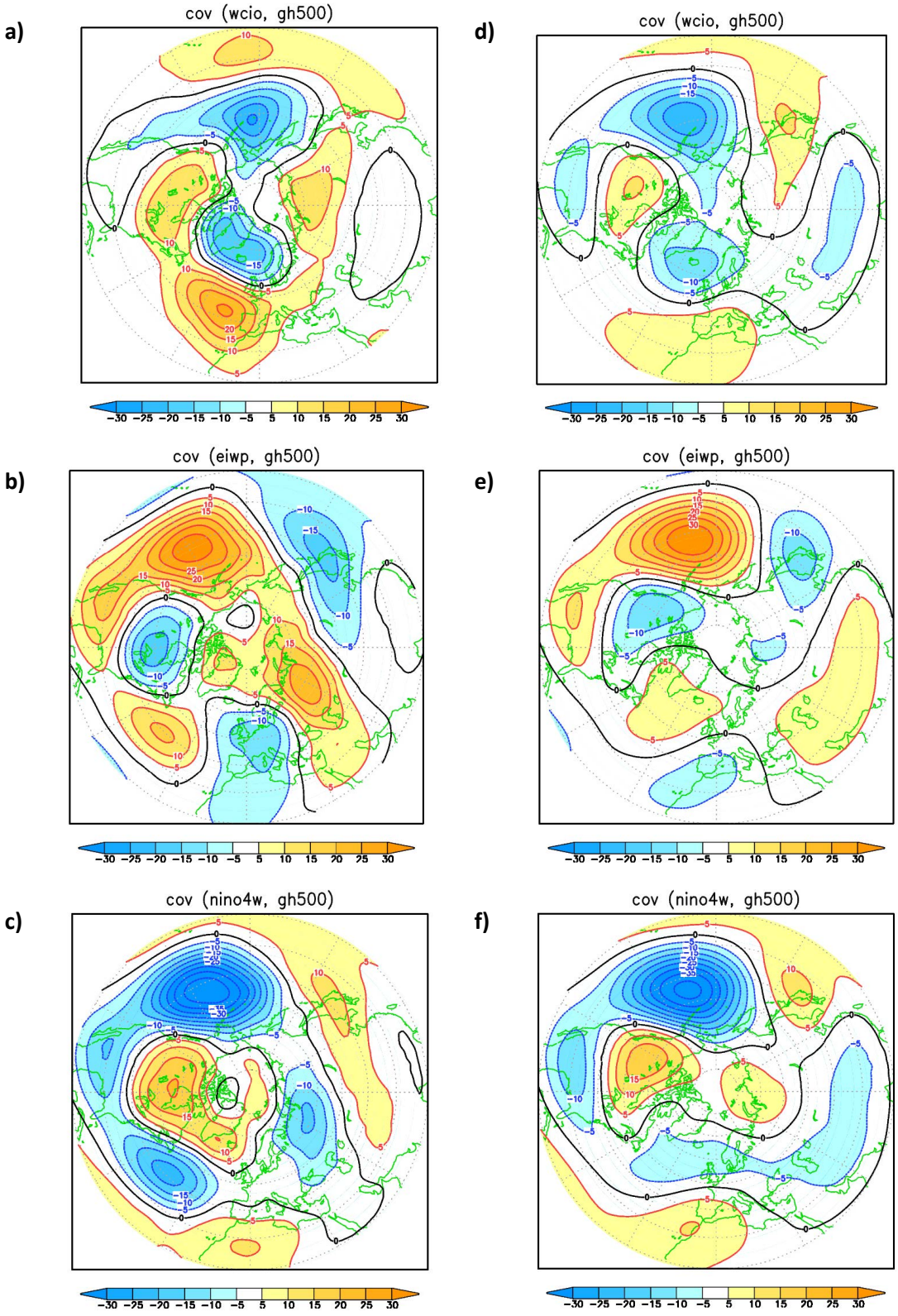

Figure 8 Covariance of DJF 500-hPa height with the stand. rainfall anomaly in the WCIO (a), EIWP (b) and NINO4W (c) regions. Data from ERA-Interim/GPCP. (d) to (f): as in (a)-(c), but from System-4.

One could interpret the results from Figs 7 and 8 by saying that covariances with SST anomalies essentially capture the signal associated with ENSO events. However, ENSO-related SST explain only a fraction of the variability in diabatic heating in the western half of the Indo-Pacific basin; here, particularly over EIWP, SST anomalies exert a relatively poor constraint over the actual sources of extratropical teleconnection. In such conditions, ensemble members for the same season (with quite similar SST) may produce different patterns of diabatic heating. When rainfall anomalies are used to trace teleconnections, the position of anomalous heat sources is properly taken into account, and the comparison between the observed and model response becomes more accurate.

With regard to the connections between WCIO and the North Atlantic variability, we noted that the NAO signal associated with positive rainfall anomalies differs substantially, in amplitude and even sign, with the corresponding signal in the SST covariances. The arguments above suggest that the association between above-average rainfall over WCIO and positive NAO is not originated by ENSO. This is confirmed by the results displayed in Fig. 9. In panel 9a, the time series of observed DJF rainfall anomalies in WCIO is shown using both original GPCP data and using only the component of the rainfall time series which is orthogonal (ie linearly un-correlated) with the SST anomalies in the NINO3.4 region (a classical ENSO indicator). Also, rainfall and 500-hPa height covariances with the ENSO-independent WCIO time series are shown, to be compared with Fig 5a and 7a respectively.

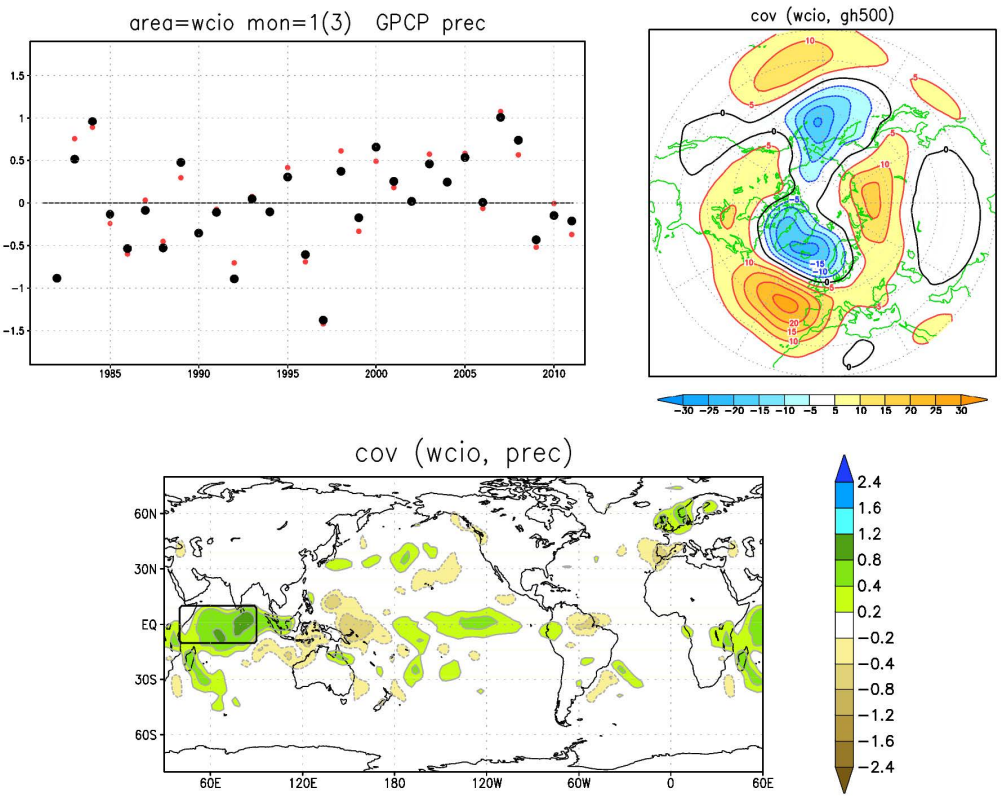

Figure 9 a) Time series of DJF rainfall in the WCIO region, from GPCP-2.2; red dots: total anomaly; black dots: anomaly orthogonal to the Nino3.4 SST time series. b) covariance of ERA-Interim 500-hPa height with the standardized black-dot time series. c) covariance of GPCP rainfall with the standardized black-dot time series.

It is evident that the total rainfall signal over WCIO, even when averaged over the whole DJF season, is mostly determined by the ENSO-independent component. If removing the ENSO component reduces the strength of the association between WCIO and central Pacific rainfall (see Fig. 9c), the positive NAO signal in the extratropical teleconnection is hardly affected, showing an identical pattern and an even slightly greater amplitude (Fig. 9b). These results do not rule out the possibility that SST anomalies in the western Indian Ocean may affect the North Atlantic Oscillation; however, such a signal does not appear to be driven by ENSO, nor it emerges as the dominant mode in the WCIO SST variability during the boreal winter.

4 Implication for predictability across time scales

In order to investigate the implications of the teleconnections described above on long-range predictability in the Atlantic-European region, three issues will be addressed in this section:

a) what skill can be achieved in predicting the inter-annual variability of Indo-West Pacific rainfall?
b) can the discrepancies between observed and modelled teleconnection patterns be attributed to sampling errors?
c) are the seasonal-scale teleconnections consistent with those detected on the sub-seasonal scale, and are they relevant to the understanding of decadal-scale variability?

4.1 Predictive skill for Indo-Pacific rainfall

Although the performance of an ensemble prediction system is best described by probabilistic scores, here we provide a basic assessment of the skill of ensemble-mean forecasts of DJF rainfall anomalies over the selected areas using the 'traditional' anomaly correlation score applied to time series of GPCP data and System-4 re-forecasts initialized on 1 November. In Fig. 10, plots comparing the observed anomaly time series (in red), the anomalies from the individual ensemble members (in green) and the ensemble-mean anomaly (in blue) are shown for the WCIO (top), EIWP (centre) and NINO4W (bottom) areas. The title above each panel shows the correlation between observed and ensemble mean anomalies; in parentheses, an estimate of "perfect-model" skill is given, defined as the average correlation between an individual ensemble member and the mean of all the other members.

If we start from the NINO4W region, the strong constraint exerted by SST on rainfall is translated into a high skill (ac = 0.91) and a strong consistency among ensemble members. The perfect-model correlation (0.95) suggests a slight under-dispersion of the ensembles, but overall the System-4 ensembles provide a reliable prediction. Moving westward, the EIWP region is also characterized by high skill (ac = 0.86) for the ensemble-mean, even higher than the perfect-model correlation of 0.76 (note that the perfect model value is an estimate of the mean correlation, not an upper limit). Since in this region the local correlation between SST and rainfall is general weak (see Fig. 2), it follows that the predictability of EIWP rainfall anomalies is likely to be originated by the dynamical response to a remote forcing. Table 1 shows that the anti-

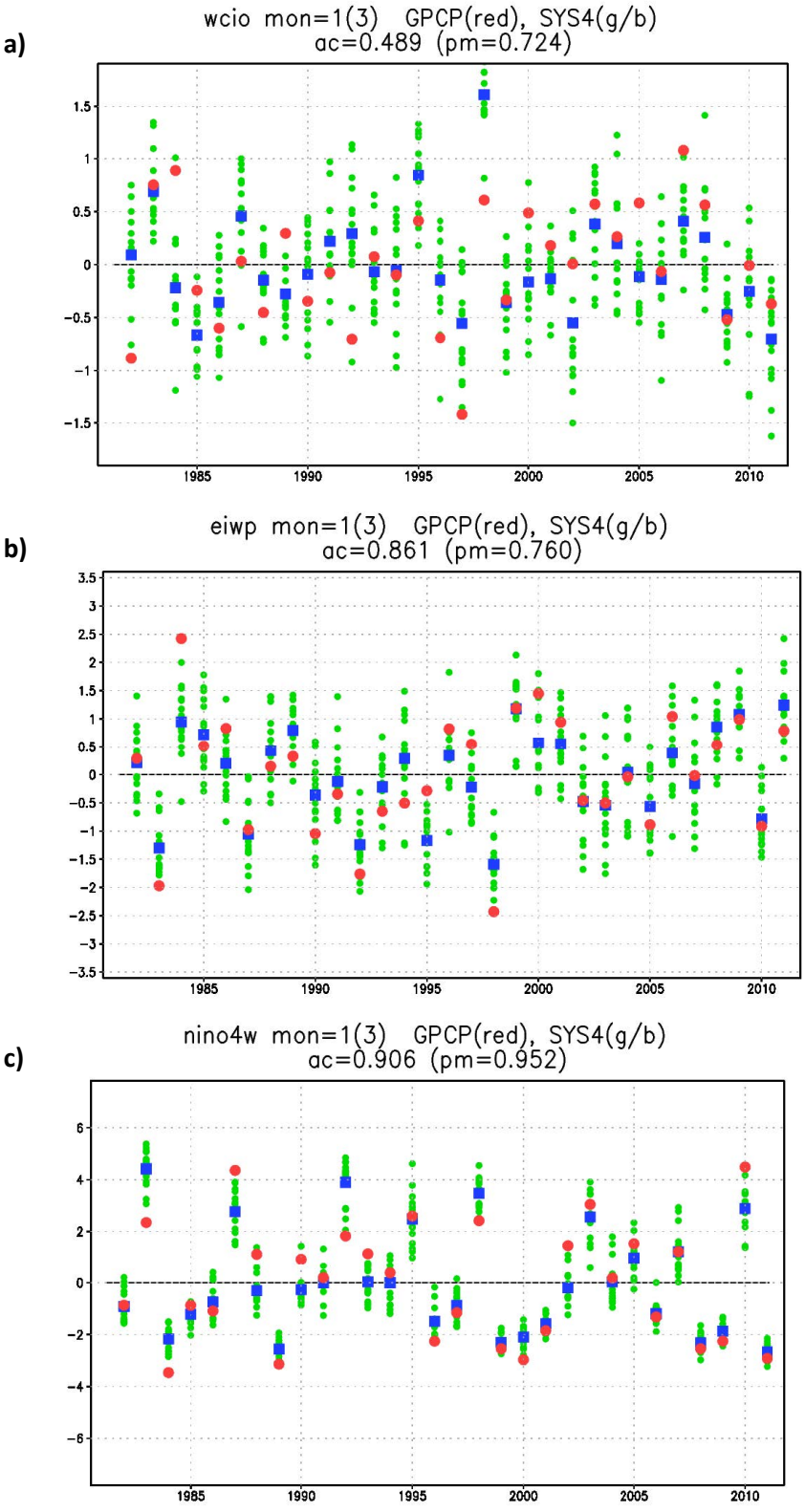

Figure 10 Time series of observed and predicted rainfall anomalies in a) WCIO, b) EIWP, c) NINO4W. Red dots: GPCP data. Blue squares: ensemble-mean from Sys-4. Green dots: individual ensemble members. AC: correlation between GPCP and ens.-mean anomalies, PM: perfect-model correlation.

correlation between rainfall in EIWP and in NINO4W is very strong and consistent between GPCP and model data (-0.82 for GPCP, -0.80 for System-4). So, the interannual variability of the EIWP rainfall is strongly linked to ENSO, and this link is realistically simulated in System-4.

For WCIO, the actual model skill drops to a correlation of 0.49, which is significantly less than the perfect-model estimate of 0.72. The ensemble system is therefore under-dispersive in this region, and it would be optimistic to take the perfect-model correlation as a reliable estimate of potential predictability. Table 1 shows that the WCIO rainfall anomalies are more strongly connected with the variability in the rest of the Indo-Pacific domain in System 4 than in the observed data. The correlation of observed WTIO rainfall with rainfall in EIWP and NINO4W is only -0.14 and 0.18 respectively, but these correlations become -0.47 and 0.51 respectively in System 4. So, the influence of ENSO-related variability in the Western Indian Ocean appears to be "over-played" by System-4. Unfortunately (for European forecasters), as shown in fig. 9, it is the ENSO-independent component of Indian Ocean rainfall which seems to drive the connection with the NAO.

4.2 Robustness of the estimated extra-tropical teleconnections

As seen by comparing panels (a) and (d) in Fig. 8, System-4 under-estimates the amplitude of the covariance between WCIO rainfall and geopotential anomalies over the North Atlantic, with respect to observations. This can be quantified by computing the correlation between WCIO rainfall anomalies and a NAO index based on sea-level pressure data (namely, the NAO index follows the traditional "Azores - Iceland" definition, but using area averages over two 30-deg-lon*15-deg-lat grid boxes instead of individual grid points). Table 1 shows that such a correlation is 0.39 for GPCP-ERA data, while drops to 0.25 for System-4.

Are these two values significantly different? Rather than using parametric tests, we can assess the robustness and significance of the correlation by computing it from one single ensemble member in the re-forecasts. Let us consider the simple case of selecting the member with the same number (1 to 15) in each of the 30 years. The top row in Table 2 shows that one-member correlations range from a minimum of -0.03 to a maximum of 0.46, with 5 out of the 15 members giving a correlation greater than 0.4 (and therefore, of the observed value). By themselves, these numbers suggest that the difference between observations and System-4 is within sampling uncertainty.

To explore the issue further, Fig. 11a and 11b show maps of covariances between 500-hPa height and WCIO rainfall analogous to the map in Fig 8d, but computed from the 5 member with either the lowest (panel a) or the highest (panel b) WCIO-NAO correlations. By construction, the Atlantic signal is much stronger in panel 11b than in 11a, although it is still not as large as in the observed covariance map (see fig. 8a). On the contrary, the low over the North Pacific is stronger when the WCIO-NAO correlation is weaker, suggesting that in System-4 the Pacific signal tends to suppress the one over the Atlantic.

	WCIO obs	EIWP obs	NAO obs	WCIO Sys4	EIWP Sys4	NAO Sys4
WCIO		-0.14	0.39		-0.47	0.25
EIWP	-0.14		-0.08	-0.47		-0.13
NINO4W	0.19	-0.82	-0.09	0.51	-0.80	0.13

Table 1. Correlations between seasonal-mean indices of rainfall anomalies in 3 Indo-Pacific regions (WCIO, EIWP, NINO4W) and a sea-level-pressure NAO index, for observational data (columns 2-4) and System-4 members (columns 5-7)

	Min	Lower tercile	Upper tercile	max
Cor (WCIO, NAO)	-0.03	0.13	0.43	0.46
Cor (WCIO, NINO4W)	0.33	0.47	0.57	0.65

Table 2. Minimum, lower tercile, upper tercile and maximum value for the correlations among selected indices, derived from individual ensemble members in the System-4 reforecasts.

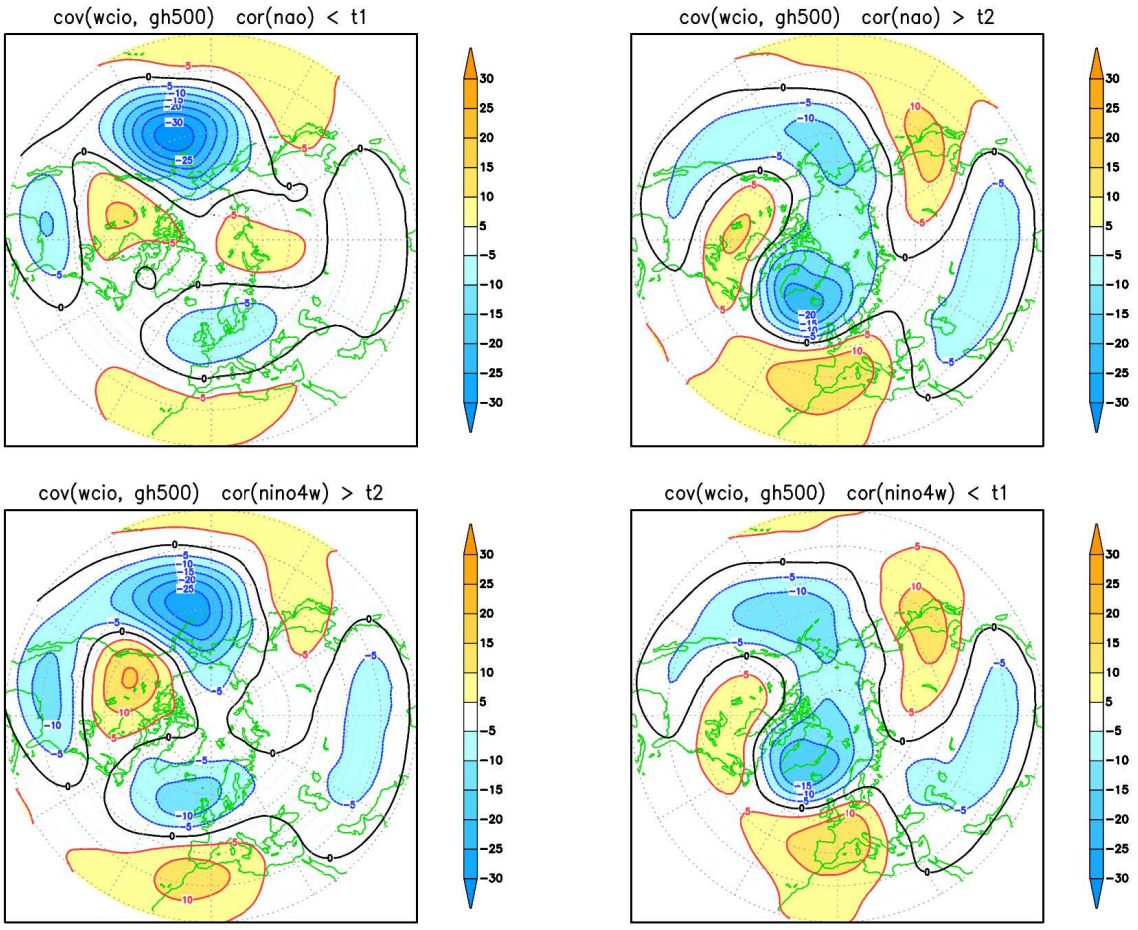

Figure 11 Top row: covariance between 500-hPa height and WCIO rainfall in Sys-4 re-forecasts, from the five ensemble members with the smallest (a, top left) and largest (b, top right) correlation between WCIO rainfall and NAO index. Bottom row: as above, but for the five ensemble members with the largest (c, bottom left) and smallest (d, bottom right) correlation between WCIO and NINO4W rainfall indices.

It this related to the too strong link between Indian and Central Pacific rainfall in System-4, which was discussed above? To verify this hypothesis, panels 11c and 11d show two additional 5-member covariance maps with WCIO rainfall, this time computed by selecting the 5 members with the strongest (ie, further from observed) WCIO-NINO4W rainfall correlation (11c) and those with the weakest (ie, closer to observed) correlation. By comparing panel 11c with 11a, and panel 11d with 11b, it is evident that a weaker link between Indian and Central Pacific rainfall favours a stronger correlation between WCIO rainfall and the NAO, at the expense of the signal in the North Pacific. Note that, in the observations, rainfall in NINO4W has a marginal negative correlation with the NAO (see Table 1 and Fig. 8c), so it is reasonable to expect that linking the WCIO and NINO4W regions would "dilute" the NAO teleconnection originated from the former region.

We commented above on the WCIO-NINO4W correlation in System 4 being much larger than in the observations. To confirm that this difference is significant, the bottom row in Table 2 shows statistics of this correlation when computed from individual ensemble members. Even the lowest single-member value (0.33) well exceeds the observed correlation (0.19), with 5 members showing correlations three-to-four times larger. In summary, although we cannot prove that System-4 has a robust systematic error in the WCIO-North Atlantic teleconnections by looking directly at WCIO-NAO correlation, we can state that the significantly stronger link between WCIO and central Pacific rainfall in System-4 is consistent with a blending of the observed teleconnections from the two tropical regions and the reduced link with NAO variability. In turn, the excessive amplitude of ENSO variability in the early part of System-4 seasonal forecasts, discussed in Molteni et al. (2011), is likely to contribute to the dominance of the ENSO signature in the distribution of Indo-Pacific rainfall.

4.3 Consistency across time scales

Another approach to assessing the robustness of the Indo-Pacific teleconnections is to investigate the consistency of the signal on different time scales. In the Introduction, studies focussing on either the intra-seasonal or the decadal time scale were mentioned. As far as statistical significance is concerned, the intra-seasonal scale has the advantage of providing a greater number of independent realizations within the period covered by reliable observational datasets than the seasonal-mean record. In addition, this timescale is highly relevant to medium- and monthly-range predictions, and the impact of reproducing the MJO teleconnection on forecast skill in such time ranges has been well documented (eg Vitart 2013).

As quoted above, a number of studies have focussed on composite anomalies associated with different MJO phases according to the Wheeler-Hendon (2004) definition. Figure 12, adapted from Vitart and Molteni (2010), shows composites of 500-hPa height anomalies occurring ten days after those classified in phases 3 of the MJO. The location of maximum increase in tropical rainfall is located over the central Indian Ocean in Phase 3, and the pattern of composite rainfall anomalies has strong similarities with the rainfall covariance map computed above from the WCIO seasonal means (Fig 8a). The left panel of Fig. 12 shows a composite computed from a set of 15-member, 46-day experiments started from during the northern winters of 1989 to

2008, using a version of the ECMWF model operational from November 2007 until June 2008; the panel on the right shows the corresponding composite from ERA-Interim data for the same winters.

In both the observed and model composites in Fig. 12, a negative anomaly centred above Alaska is occurs together with a positive NAO dipole, in agreement with the seasonal-mean teleconnection from the WCIO region in Fig. 8a. Positive anomalies occur at mid-latitudes over in both the Euro-Atlantic and North-Pacific sectors, while a third, weaker negative centre is located to the east of the Caspian Sea. Compared with observations, the model over-emphasizes the Pacific component of the signal with respect to the Atlantic anomalies, with an evident underestimation of the positive centre in the NAO dipole. It should be mentioned that MJO composites produced with more recent versions of the ECMWF model produce a closer similarity to the observed teleconnection.

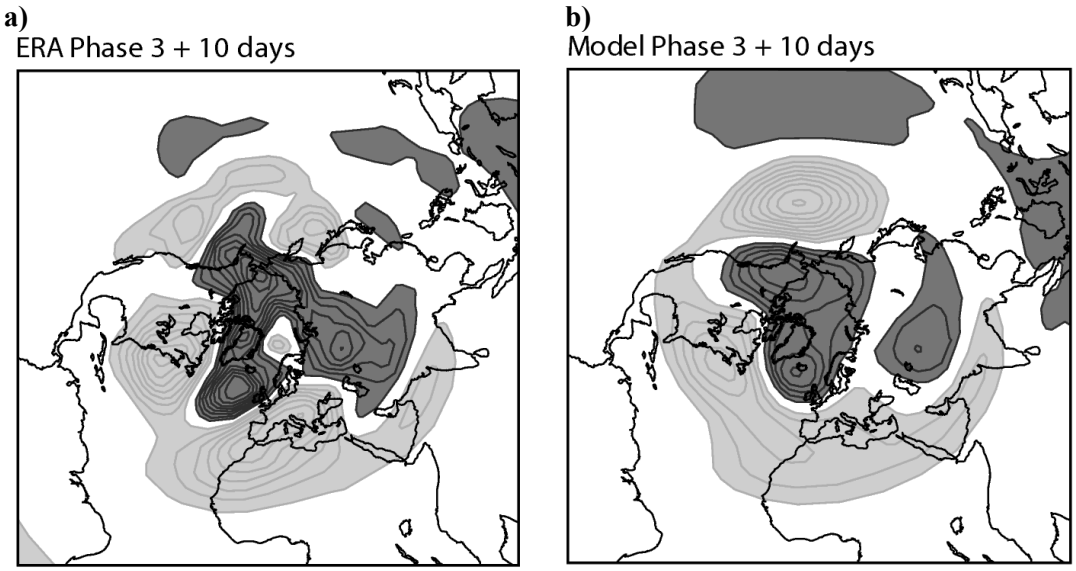

Figure 12 Composites of 500-hPa height anomalies occurring ten days after tropical anomalies classified in MJO phase-3. a) from ERA-Interim. b) from 45-day runs of the ECMWF model. Reproduced from Vitart and Molteni (2010).

Here, we mainly want to stress that the Alaskan low - positive NAO combination can be consistently detected on both intra-seasonal and inter-annual time scales in association with increased rainfall in the western and central Indian Ocean. Also, the intraseasonal diagnostics confirm that, in observations, the North Atlantic component of the teleconnection is at least as strong as the North Pacific one. This is consistent with the observed signal in seasonal-mean data, suggesting that the differences detected between System-4 and ERA-GPCP teleconnections are unlikely to be originated by sampling errors in the observed seasonal-mean record.

Turning now to the decadal scale, it is interesting to note that the sign of the North Pacific and North Atlantic anomalies detected in the WCIO rainfall and MJO-Phase-3 teleconnections are also reproduced in the inter-decadal differences in 500-hPa geopotential height between the last two quarters of the 20th century (namely, 1976-2000 minus 1951-1975), shown in Fig. 13a. A number of studies have been published, in which AGCMs have been used to investigate the response to the interdecadal change

in SST during the same period (see Fig. 13b), and specifically the possible link between the warming of tropical Indian Ocean and the shift towards positive NAO anomalies in the latter part of the 20th century (e.g. Hurrell et al. 2004, Hoerling et al. 2004, Sanchez-Gomez et al. 2008) The general conclusion from these studies is that the geopotential change pattern can be reasonably well simulated, but with an amplitude reduced to approximately half of the observed signal.

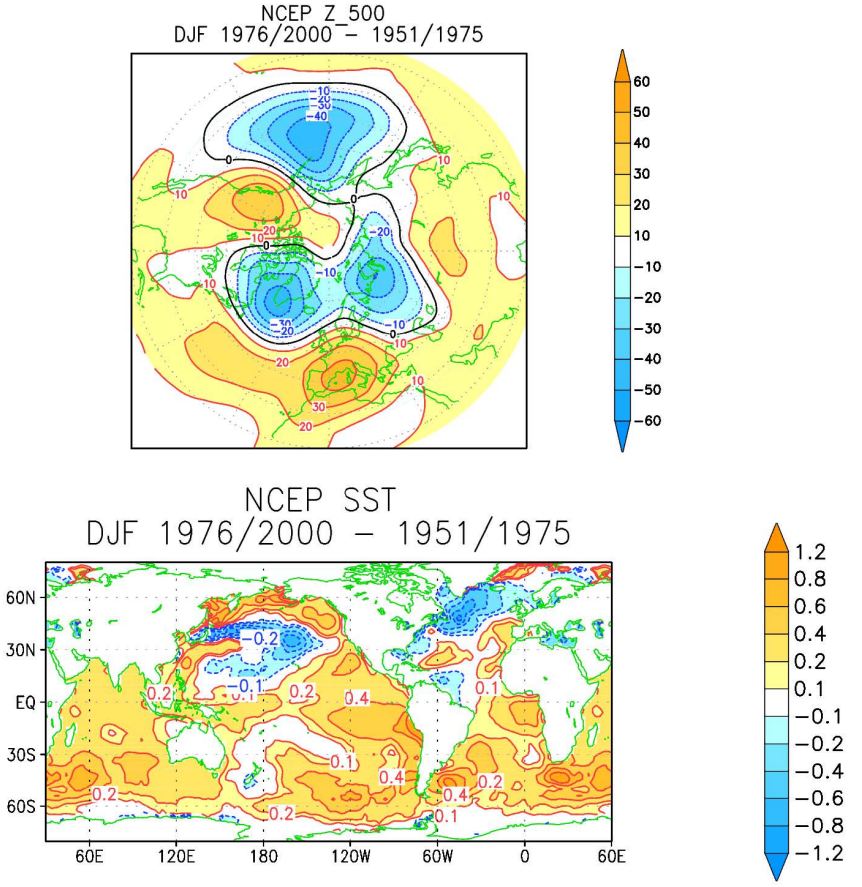

Figure 13 Differences between averaged fields in DJF 1976-to-2000 and 1951-to-1972. a) 500-hPa height, from the NCEP re-analysis (Kalnay et al. 1996). b) SST from Smith and Reynolds (2003).

Although the difference could, again, be due to sampling issues associated with internal variability, two elements suggest that other factors are likely to play a role. Firstly, distributions of NAO changes from individual ensemble members (such as the one shown by Hurrell et al. 2004, and reproduced here in Fig. 14a, show that the observed NAO change exceeds simulated value in almost the totality of the model realizations. Secondly, the reduction in the modelled NAO signal is of the same order of magnitude of that detected in the System-4 teleconnections from WCIO rainfall.

In the previous sections, we have argued that the System-4 reduction is consistent with an incorrect (in this case, too strong) link between rainfall anomalies in different portions of the Indo-Pacific basin. A similar argument can be invoked to explain the reduced inter-decadal NAO response in AGCM experiments. In such experiments, a warming trend is specified in the SST covering both the WCIO and most of the EIWP region. However, AGCM cannot reproduce the negative feedbacks, associated with

changes in solar radiation and evaporation, which contribute to the negative SST-rainfall correlation occurring over most of the EIWP domain (see fig. 2). Therefore, the typical AGCM response to a zonally uniform SST increase in the Indian and west Pacific domain is a zonally- coherent increase in precipitation near the Equator, although with a minimum in the EIWP region (see the multi-model result from Hoerling et al. 2004, reproduced here in Fig. 14b).

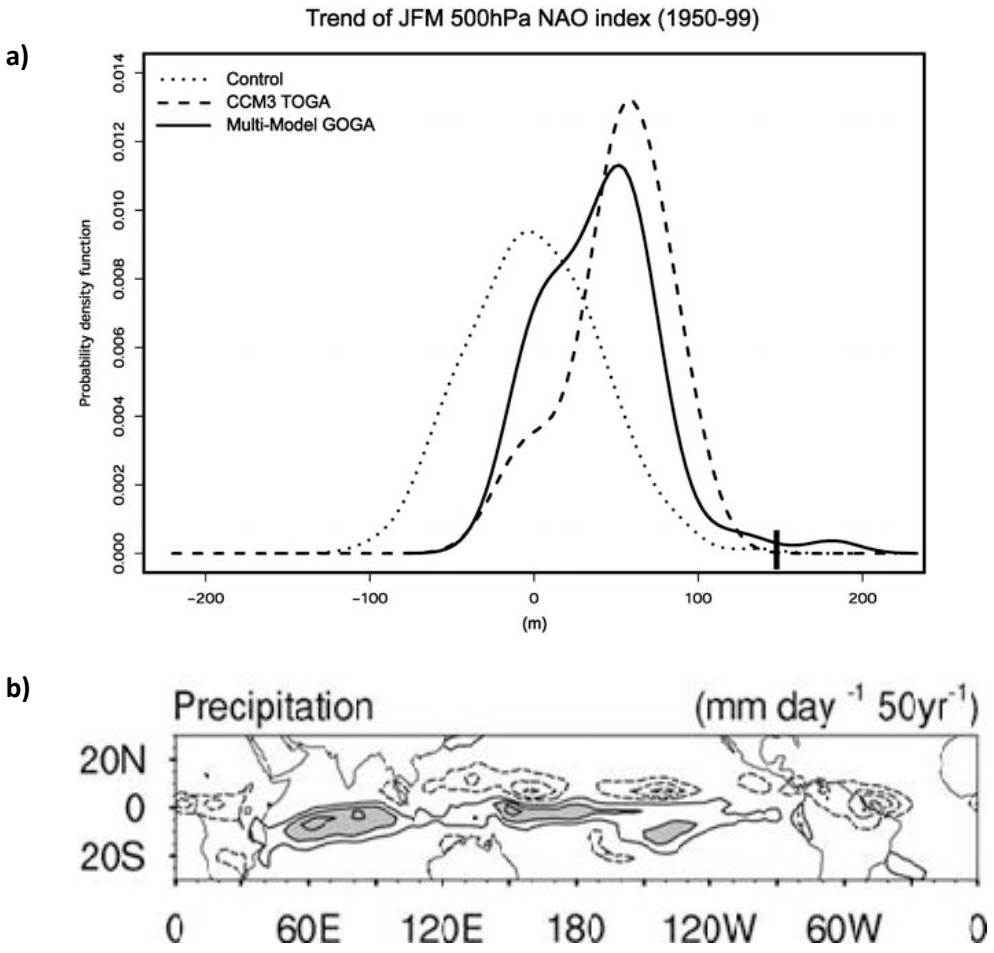

Figure 14 a) Distribution of 1950-to-1999 NAO trends from the AGCM ensemble experiments described in Hurrell et al. 2004. Black bar: observed value. The NAO index is based on 500-hPa height anomalies. b) Multi-model ensemble-mean trend of precipitation for the same experiments and period, as reported in Hoerling et al. (2004).

On the other hand, observed cloud cover data presented by Deser and Phillips (2006) and the sea-level-pressure analysis of Copsey et al. (2006) are not consistent with a increasing rainfall trend in EIWP. Since the sign of the extratropical teleconnections from WCIO and EIWP rain are opposite over both the North Pacific and the Euro-Atlantic sectors according to seasonal-mean data (see Fig.8), the typical AGCM combination of positive rainfall trends in both the WCIO and EIWP region would reduce the amplitude of the combined extra-tropical response with respect to a situation where the EIWP trend would be absent or negative.

One may argue that the seasonal-mean record is dominated by ENSO variability, and it may not provide a good "proxy" for decadal-scale teleconnections. However, by considering only the component of times series orthogonal to Nino3.4 SST, we showed

in Fig. 9 that the WCIO teleconnections are almost unaffected by the ENSO signal. By applying the same technique to observed SST data, and computing the covariance of rainfall with the average SST in the combined WCIO + EIWP region (40-140E, 10N-10S), we find again a tri-polar pattern with positive rainfall anomalies in WCIO and negative ones in EIWP (Fig. 15), even if the associated SST anomalies are positive in both regions (as in the decadal trend of Fig. 13b).

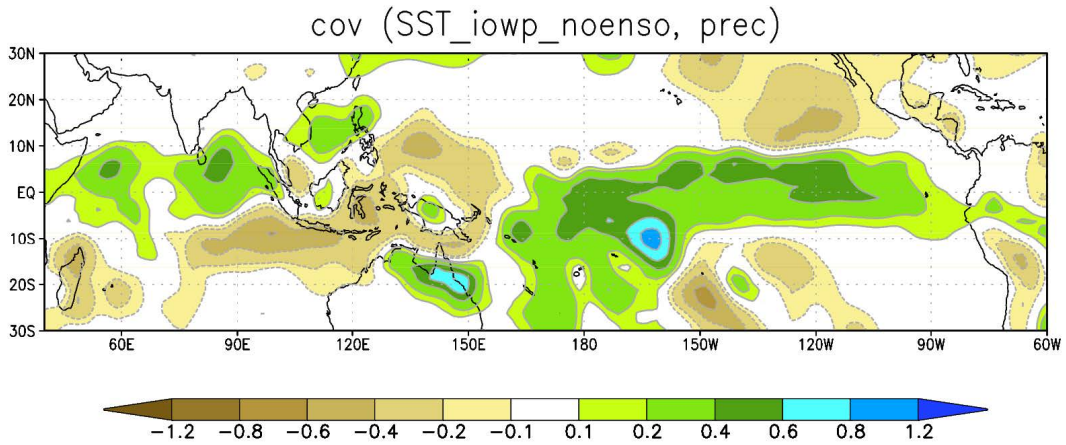

Figure 15 Covariance of GPCP rainfall anomalies with the time series of SST averaged in a combined Indian Ocean - West Pacific domain (40-140W, 10N-10S), after removal of the anomaly component correlated with the Nino3.4 SST.

5 Summary and conclusions

The main messages conveyed by our investigation of Indo-Pacific teleconnections in observed and coupled-model records can be summarized as follows.

- Teleconnections originated from the tropical Indian and West Pacific Oceans cannot be simply understood on the basis of a direct forcing of atmospheric heat sources by local SST anomalies. In the western portion of the Indo-Pacific domain (typically, west of 140W), local correlations between SST and rainfall are either weaker than in the central Pacific, or even negative. In this respect, a different behaviour between the western and eastern part of the Indian Ocean should be taken into account during the northern winter, even if a dipolar structure in SST (evident during autumn) can no longer be detected.
- Because of the weaker constraint of SST on rainfall discussed above, teleconnections diagnosed as a function of SST anomalies in the Indian and West Pacific Oceans fail to adequately represent the response to anomalous atmospheric heat sources in these regions. Instead, if teleconnections are computed from covariances with rainfall anomalies, a stronger consistency is found both between observed and modelled patterns, and between diagnostics derived from seasonal and intra-seasonal time scales.
- The main mode of variability in Indo-Pacific rainfall associated with planetary-scale teleconnections is a tri-polar structure with two positively correlated centres in the Western Indian Ocean and the Central Pacific, and a third centre around the Maritime Continents which is anti-correlated with the other two.

This mode can be forced by ENSO, but is also found in MJO composites and seasonal means where the linear ENSO signal is removed.

- Positive rainfall anomalies in the Western and Central Indian Ocean are connected with a negative height anomaly centred over Alaska and a positive NAO signal, in a combination reminiscent of the Cold-Ocean-Warm-Land pattern of Wallace et al. (1996). This teleconnection does not appear to be driven by the ENSO-forced component of Indian Ocean rainfall, and is consistent with MJO teleconnections found in previous studies.
- System-4 underestimates the link between Western-to-Central Indian Ocean (WCIO) rainfall and the NAO with respect to observations. Although a large variability is found among different ensemble members in this respect, it was shown that this discrepancy is linked to a significant positive bias in the correlation between rainfall in the WCIO and NINO-4 regions, which weakens the NAO component in the combined teleconnection. This suggests that an incorrect relationship between rainfall in different portions of the Indo-Pacific basin may also account for the underestimation of inter-decadal signals in AGCM simulations.

When the teleconnection patterns diagnosed from observed and System-4 data are compared (using rainfall as the "source" variable), one may conclude that in most cases the coupled model does a quite realistic job, and progress with respect to previous-generation seasonal forecast systems is evident. Still, on one crucial aspect relevant to predictions for Europe, ie the link between NAO and tropical rainfall, System-4 simulations are still unsatisfactory. As we discussed above, such a link is difficult to reproduce across a range of time scales, ranging from the intra-seasonal to the decadal.

If ENSO is not the main driver of Indo-Pacific links with the NAO, can such links be predictable on the seasonal scale? What factors should be properly modelled? Looking at the strength of the MJO-related signal on intra-seasonal time-scale, one possible line of investigation concerns the non-linear aspects of the MJO response. Composites in opposite MJO phases may look symmetric, but the atmosphere may not spend the same amount of time in each phase: the propagation speed may be affected by the atmospheric moisture content, or by the intensity of ocean-atmosphere feedbacks in region with different mixed-layer depth. And the same anomaly in the atmospheric heat source will generate a different Rossby wave source depending on the local vorticity gradient (Sardeshmuhk and Hoskins 1988). So, even if the exact MJO phase may not be predictable beyond one-to-two months, the non-linear 'residual' of a MJO cycle might be affected by the seasonal (or decadal) components of climate variability.

In conclusion, we have argued that the main dynamical aspects of Indo-Pacific teleconnections are consistent and relevant for weather and climate predictions on a wide range of scales. It is possible that factors affecting the simulation of inter-decadal trends may be effectively diagnosed from simulations spanning the time of a typical MJO cycle. If this is the case, the recent surge in interest for sub-seasonal predictions (eg Vitart et al. 2012) can have a positive impact for a wider community of climate scientists, and lead to better seasonal and decadal forecasts.

Acknowledgements

The authors are grateful to all ECMWF staff involved in the development and operational implementation of System-4. In particular, the contribution of M. Balmaseda, K. Mogensen and L. Ferranti is acknowledged and appreciated.

References

Anderson, D. L. T., E. S. Sarachik, P. J. Webster, and L. M. Rothstein (eds), 1998: The TOGA Decade: Reviewing the Progress of El Niño Research and Prediction, J. Geophys. Res., 103(C7), 14167–14510, doi:10.1029/98JC00112.

Annamalai, H.., H. Okajima, and M. Watanabe, 2007: Possible impact of the Indian Ocean SST on the Northern Hemisphere circulation during El Niño. J. Climate, 20, 3164–3189.

Balmaseda M.A., Mogensen K., A. Weaver, 2013: Evaluation of the ECMWF Ocean Reanalysis ORA-S4. Quarterly J. Roy. Met. Soc. In press.

Cassou, C., (2008), Intraseasonal Interaction between the Madden-Julian Oscillation and the North Atlantic Oscillation." *Nature* 455, no. 7212: 523-27.

Copsey, D., Sutton, R. and Knight, J.R. (2006). Recent trends in sea level pressure in the Indian Ocean region. Geophysical Research Letters 33: doi: 10.1029/2006GL027175.

Dee, D. P., and co-authors, 2011: The ERA-Interim reanalysis: configuration and performance of the data assimilation system. Quart. J. R. Meteorol. Soc., 137, 553-597.

Deser, C., and A. S. Phillips, 2006: Simulation of the 1976/1977 climate transition over the North Pacific: Sensitivity to tropical forcing. J. Climate, 19, 6170-6180.

Hoerling M.P., J. W. Hurrell , T. Xu , G. T. Bates, and A. Phillips, 2004: Twentieth Century North Atlantic climate change. Part II: Understanding the effect of Indian Ocean warming. Climate Dyn. 23, 391-405.

Hurrell, J.W., Hoerling, M.P., Philliphs, A.S. and Xu, T., 2004. Twentieth century North Atlantic climate change. Part I: Assessing determinism“. Climate Dynamics 23: 371–389.

Kalnay, E., and Coauthors, 1996: The NCEP/NCAR 40-Year Reanalysis Project. Bull. Amer. Meteor. Soc., 77, 437–471.

Kucharski, F., Molteni, F., and Bracco, A., 2006: Decadal interactions between the Western Tropical Pacific and the North Atlantic Oscillation. Climate Dyn., 26, pp. 79-91, doi: 10.1007/s00382-005-0085-5

Lin. H., G. Brunet and J. Derome, 2009: An Observed Connection between the North Atlantic Oscillation and the Madden-Julian Oscillation. J. Climate, 22, 364-380.

Madec G. 2008. NEMO reference manual, ocean dynamics component: NEMO-OPA. Note du Pole de Modelisation 27, Institut Pierre-Simon Laplace (IPSL), France.

Molteni, F., T. Stockdale, M. Balmaseda, G. Balsamo, R. Buizza, L. Ferranti, L. Magnusson, K. Mogensen, T. Palmer and F. Vitart, 2011: The new ECMWF seasonal forecast system (System 4). ECMWF Technical Memorandum no. 656.

Saji, N.H., B.N. Goswami, P.N. Vinayachandran, and T. Yamagata. 1999. A dipole mode in the tropical Indian Ocean. Nature 401:360–363.

Sanchez-Gomez, E., C. Cassou, D. L. R. Hodson, N. Keenlyside, Y. Okumura, and T. Zhou, 2008: North Atlantic weather regimes response to Indian-western Pacific Ocean warming: A multi-model study. Geophys. Res. Lett., 35, L15706, doi:10.1029/ 2008GL034345.

Sardeshmukh, P. D. and B. J. Hoskins (1988) The generation of global rotational flow by steady idealized tropical divergence. J. Atmos. Sci., 45, 1228–1251.

Schott, F. A., S.-P. Xie, and J. P. McCreary Jr. (2009), Indian Ocean circulation and climate variability. Rev. Geophys., 47, RG1002, doi: 10.1029/2007RG000245.

Smith, T. M. and R. W. Reynolds, 2003: Extended Reconstruction of Global Sea Surface Temperatures Based on COADS Data (1854-1997). J. Climate, 16, 1495-1510.

Valcke, S., 2013: The OASIS3 coupler: a European climate modelling community software, Geosci. Model Dev., 6, 373-388, doi:10.5194/gmd-6-373-2013

Vitart, F., 2013: Evolution of ECMWF sub-seasonal forecast skill scores over the past 10 years. ECMWF Technical Memorandum no. 694.

Vitart, F. and Molteni, F. (2010), Simulation of the Madden– Julian Oscillation and its teleconnections in the ECMWF forecast system. Q.J.R. Meteorol. Soc., 136: 842–855. doi: 10.1002/qj.623

Vitart, F., A.W. Robertson and D.L.T. Anderson, 2012: Subseasonal to seasonal prediction project, 2012: Bridging the gap between weather and climate. WMO Bulletin, 61(2), 23-28.

Wallace JM, Zhang Y, Bajuk L (1996) Interpretation of interdecadal climate trends in Northern Hemisphere surface air temperature. J Clim 9:249–259

Wang, B., Ding, Q., Fu, X., Kang, I.-S., Jin, K., Shukla, J. and Doblas-Reyes, F.J. (2005). Fundamental challenge in simulation and prediction of summer monsoon rainfall. Geophysical Research Letters, 32, L15711. DOI: 10.1029/2005GL022734.

Webster, P. J., A. M. Moore, J. P. Loschnigg, and R. R. Leben, 1999: Coupled Ocean-Atmosphere Dynamics in the Indian Ocean During 1997-98. Nature 401, no. 6751: 356-60.

Wheeler, M. C., H. H. Hendon, 2004: An All-Season Real-Time Multivariate MJO Index: Development of an Index for Monitoring and Prediction. Mon. Wea. Rev., 132, 1917–1932.